IEEE Access
Multidisciplinary | Rapid Review | Open Access Journal

SPECIAL SECTION ON MULTIPHASE FLOW MEASUREMENT: TECHNIQUES AND APPLICATIONS

Received April 15, 2017, accepted May 31, 2017, date of publication June 9, 2017, date of current version August 14, 2017.

Digital Object Identifier 10.1109/ACCESS.2017.2713834

Sensitivity Distribution of CCERT Sensor Under Different Excitation Patterns

ZHEN XU, YANDAN JIANG, BAOLIANG WANG, ZHIYAO HUANG, HAIFENG JI, AND HAIQING LI

State Key Laboratory of Industrial Control Technology, College of Control Science and Engineering, Zhejiang University, Hangzhou 310027, China

Corresponding author: Baoliang Wang (blwang@iipc.zju.edu.cn)

This work was supported in part by the National Nature Science Foundation of China under Grant 61371161.

ABSTRACT This paper focuses on the study of sensitivity distribution of the capacitively coupled electrical resistance tomography (CCERT) and the influences of excitation patterns on sensitivity distributions. The sensitivity distributions of a 12-electrode CCERT sensor under three excitation patterns (the one-electrode excitation pattern, the three-electrode excitation pattern, and the five-electrode excitation pattern) are investigated and compared. The simulation study was implemented by the COMSOL Multiphysics FEM simulation software and MATLAB. The research results show that there is no negative region in the sensitivity distributions of the CCERT sensor and all the sensitivity distributions are not uniform. The research results also indicate that as the number of excitation electrodes increases, the sensitivity distributions have higher average sensitivity and better distribution uniformity.

INDEX TERMS Process tomography, electrical tomography, capacitively coupled electrical resistance tomography (CCERT), excitation pattern, sensitivity distribution.

I. INTRODUCTION

Electrical tomography (ET), which includes electrical resistance tomography (ERT), electrical capacitance tomography (ECT) and electromagnetic tomography (EMT), has become popular since 1980s [1]–[4]. Due to its advantages of low cost, non-intrusive, high speed, no radiation hazard and being suitable for various sizes of pipes, ET has received great attentions from scientists and engineers and many achievements/technical progresses have been obtained [1]–[10]. Now, ET is an attractive and important technique in the research field of multiphase flow measurement [5]–[10].

Using simulation software to study the sensitivity distribution of ET and the influence of measurement strategy (excitation and detection patterns) on the sensitivity distribution is an essential work which plays an important role in sensor design, image reconstruction and parameter measurement of ET [9]–[15]. Many research works have been undertaken and many excellent results have been obtained. For ERT, the most popular measurement strategy of traditional ERT is the adjacent strategy, which excites with current signal and detects the voltage between each pair of adjacent electrodes. This approach provides high sensitivity near the pipe/vessel wall but poor sensitivity in the central region [9], [16]. Dickin and Wang [16] employed an opposite strategy (exciting opposite electrode pairs) which was less sensitive to conductivity changes than the adjacent strategy at the boundary and yielded a relatively good distinguishability due to the even distribution of currents. Wang *et al.* [18] proposed a conducting boundary strategy for the conducting vessel wall to overcome the grounding effect. Zhu *et al.* [19] studied an adaptive current excitation strategy with 32 driving electrodes and 32 voltage measurement electrodes. This method had the potential for improving qualified tomography results. Gevers *et al.* [20] increased the measurement rate of an EIT system by using parallel excitation of coded signals. Adler *et al.* [21] analyzed various choices of excitation and measurement patterns under the constraint of pair drive and noted that adjacent patterns were harmful and should be abandoned. Xiao *et al.* [22] proposed a finite element mesh optimization method to improve the ill-posedness of the traditional sensitivity matrix in ERT. Similarly, for ECT (The measurement approach is usually to excite a drive electrode with alternating current (AC) voltage signal and detect the current of remaining electrodes.) and EMT (The main approach is the single frequency sinusoidal excitation.), a lot of meaningful research works have been undertaken and useful references have been obtained [23]–[31]. Undoubtedly, all the above research results greatly enhance the development of ET and provide useful references for further research [8], [9], [14], [15].

Among the above three kinds of ET, ERT is an effective approach to qualitatively or quantitatively measure the spatial conductivity distribution of gas-liquid two-phase flow [6]–[10], [14], [15]. However, although ERT has many advantages (e.g., high speed, low cost, etc.), the measurement principle of ERT is on the basis of contact conductivity measurement [3], [9], [14]. The electrodes of ERT are directly in contact with the conductive fluid. That may result in electrochemical erosion effect and polarization effect of the electrodes. Meanwhile, if the electrodes are contaminated, unpredictable measurement errors may arise. These drawbacks more or less limit the practical application of ERT systems [5], [32], [33].

By referring to the basic idea of the capacitively coupled contactless conductivity detection (C^4D), i.e., using two coupling capacitances to form an AC measurement path and hence to realize the conductivity measurement contactlessly, a new kind of ET, capacitively coupled electrical resistance tomography (CCERT), is proposed in 2013 [32]–[34]. CCERT can be regarded as an improvement of ERT and it is a contactless measurement technique. The electrodes of CCERT are not in contact with the fluid. Thus, the drawbacks of ERT (e.g., electrochemical erosion effect, polarization effect and the influence of electrode contamination on the measurement results, etc.) can be overcome. Unfortunately, as a new kind of ET, the research on sensitivity distributions of CCERT and the influence of measurement strategy on sensitivity distribution are limited. More research works should be undertaken.

The aim of this work is to study the sensitivity distributions of CCERT and the influence of excitation patterns on sensitivity distribution by software simulation, and to obtain useful knowledge and experience for sensor design, image reconstruction and process application of CCERT.

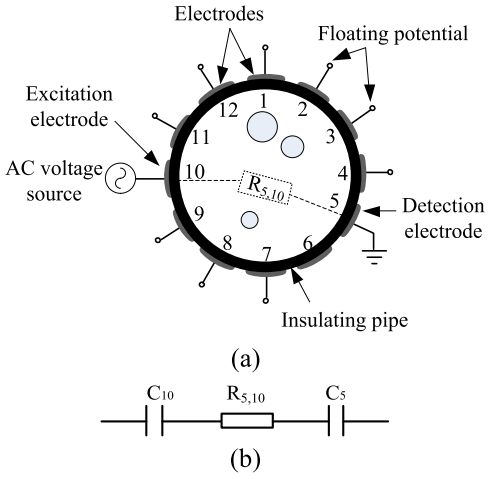

FIGURE 1. Measurement principle of a 12-electrode CCERT sensor. (a) Construction of sensor. (b) Equivalent circuit of an electrode pair.

II. EXCITATION PATTERNS AND SIMULATION MODEL

A. EXCITATION PATTERNS

Fig. 1 shows the measurement principle of a 12-electrode CCERT sensor. The electrodes are positioned equidistantly around the outer boundary of the pipe wall. For each electrode pair, the two electrodes, the insulation pipe and the conductive liquid in the pipe can form two coupling capacitances, and the conductive liquid can be equivalent to a resistor. So, the circuit between any electrode pair can also be simplified as two coupling capacitors and one resistor. Fig. 1(b) shows the equivalent circuit of the measurement electrode pair (electrode 5 and electrode 10), where C_5 is the coupling capacitance formed by electrode 5, the insulation pipe and the conductive fluid in the pipe. C_{10} is the coupling capacitance formed by electrode 10, the insulation pipe and the conductive fluid in the pipe. $R_{5,10}$ is the equivalent resistor of the fluid between the two electrodes. When the AC voltage is applied on the excitation electrode, the AC current which reflect the information of the conductivity distribution can be measured from the detection electrode.

Using the 12-electrode CCERT sensor, three excitation patterns of CCERT are investigated in this work.

The first pattern is the one-electrode excitation pattern, i.e., the one-electrode excitation and one-electrode detection pattern. In every measurement cycle, two of the electrodes are selected as the measurement electrode pair (one is the excitation electrode and the other is the detection electrode), as shown in Fig. 2(a). The excitation electrode is connected with an AC excitation voltage source, the detection electrode is kept at ground potential, while the remaining electrodes are kept at floating potential. For the one-electrode excitation pattern, there are six typical positions of the detection electrode relative to the excitation electrode, i.e., there are six typical sensitivity distributions. For an example, taking electrode 1 the excitation electrode, electrode pair 1-2, 1-3, 1-4, 1-5, 1-6 and 1-7 are the six typical measurement pairs. In one measurement cycle, electrode 1 is firstly excited and electrode 2∼12 are selected as the detection electrodes respectively to obtain the resistances of the fluid between electrode 1 and the other eleven electrodes. Then, the electrode 2∼11 are excited in sequence, so the resistances of the fluid of all single electrode pairs are measured, and so on.

The second pattern is the three-electrode excitation pattern, i.e., the three-electrode excitation and one-electrode detection pattern. Three adjacent electrodes are selected as the excitation electrodes, as shown in Fig. 2(b). For the three-electrode excitation pattern, there exist five typical sensitivity distributions corresponding to five typical positions of the detection electrode relative to the three excitation electrodes (such as electrode group 1,2,3-4, 1,2,3-5, 1,2,3-6, 1,2,3-7 and 1,2,3-8 when electrode 1, 2 and 3 are the three excitation electrodes).

The third pattern is the five-electrode excitation pattern, i.e., the five-electrode excitation and one-electrode detection pattern, as shown in Fig. 2(c). Five adjacent electrodes are selected as the excitation electrodes. Similarly, for the five-electrode excitation pattern, there exist four typical sensitivity distributions corresponding to four typical positions of the detection electrode relative to the five excitation electrodes (such as electrode group 1,2,3,4,5-6, 1,2,3,4,5-7,

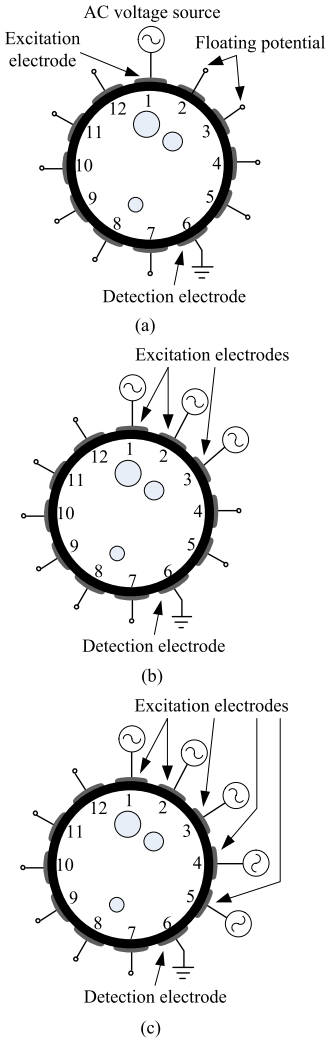

FIGURE 2. The investigated excitation patterns. (a) One-electrode excitation pattern. (b) Three-electrode excitation pattern. (c) Five-electrode excitation pattern.

1,2,3,4,5-8 and 1,2,3,4,5-9 when electrode 1, 2, 3, 4 and 5 are the five excitation electrodes).

B. SIMULATION MODEL

The sensing field of the CCERT sensor in Fig. 1 can be regarded as a quasi-static electromagnetic field, which satisfies the Maxwell's equations [10], [12], [35]. Meanwhile, to simplify the model, the fringe effect caused by the finite electrode length is neglected. Thus, the simulation model in this work is [33], [34]:

$$\begin{cases} \nabla\cdot((\sigma(x,y)+j\omega\varepsilon(x,y))\nabla\phi(x,y))=0 & (x,y)\subseteq\Omega \\ \phi_a(x,y)=V_0 & (x,y)\subseteq\Gamma_a \\ \phi_b(x,y)=0 & (x,y)\subseteq\Gamma_b \\ \dfrac{\partial\phi_c(x,y)}{\partial\vec{n}}=0 & (x,y)\subseteq\Gamma_c,(c\neq i,j) \end{cases} \tag{1}$$

where, $\sigma(x,y)$ and $\varepsilon(x,y)$ are the spatial conductivity distribution and the spatial permittivity distribution. $\phi(x,y)$ is the spatial potential distribution. $\omega = 2\pi f$ and V_0 are the angular frequency and the amplitude of the excitation AC voltage source, f is the frequency of the AC voltage source. $\Gamma_1, \Gamma_2, \Gamma_3, \ldots, \Gamma_{12}$ represent the spatial locations of the 12 electrodes. $\vec{n}$ denotes the outward unit normal vector. a, b and c are the indexes of the excitation electrode, the detection electrode and the floating electrode, respectively.

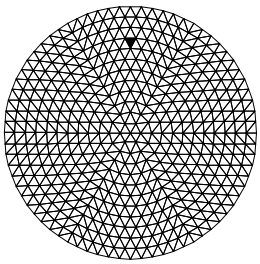

FIGURE 3. The simulation area being meshed into 864 elements.

With the simulation model in Eq. (1), the sensitivity distribution of the sensor under specific measurement strategy can be obtained by introducing the widely used finite element method (FEM) [11]–[13], [16], [17]. The simulation works were carried out by the COMSOL Multiphysics FEM simulation software and MATLAB. The simulation area of the CCERT sensor was meshed into 864 triangle elements, as shown in Fig. 3. The inner diameter of the CCERT sensor was 0.11 m and the electrode angle was 25°. The excitation frequency and the amplitude of the AC voltage source were 200 kHz and 1.0 V, respectively. The tap water with the conductivity $\sigma_0 = 0.012$ S/m and the air/gas with the conductivity $\sigma_1 = 0.0$ S/m were selected as the two phases.

During the simulation process, the excitation voltage applied to the excitation electrode(s) is known and the current on the detection electrode can be calculated by the software according to Eq. (2).

$$I_{a-b} = \int_{\Gamma_b} J_{a-b}\, d_{\Gamma_b} \tag{2}$$

where, $a-b$ is the electrode pair. J_{a-b} is the current density around the detection electrode and Γ_b is the surface area of the detection electrode. So, for the electrode pair $a-b$, the equivalent resistance R_{a-b} of the measured fluid between the excitation electrode(s) and the detection electrode can be calculated by

$$R_{a-b} = Re(V_0/I_{a-b}) \tag{3}$$

The resistance sensitivity of the ith element (for instance, the element filled in black in Fig. 3) of the electrode pair $a-b$ is defined as

$$S^i_{a-b} = \frac{R^i_{a-b} - R^0_{a-b}}{R^0_{a-b}}\mu_i \tag{4}$$

where, R^0_{a-b} represents the equivalent resistance between electrode pair $a-b$ when the pipe is full of continuous medium ($\sigma = \sigma_0$). R^i_{a-b} is the equivalent resistance between electrode pair $a-b$ when the conductivity of the ith element

changes from σ_0 to σ_1 and the remaining elements are still kept at σ_0. μ_i is the area ratio of the whole pipe cross section to the ith element.

III. SIMULATION RESULTS

A. TYPICAL SENSITIVITY DISTRIBUTIONS OF CCERT SENSOR UNDER ONE-ELECTRODE EXCITATION PATTERN

For the conventional one-electrode excitation pattern, the six typical sensitivity distributions of the CCERT sensor are shown in Fig. 4.

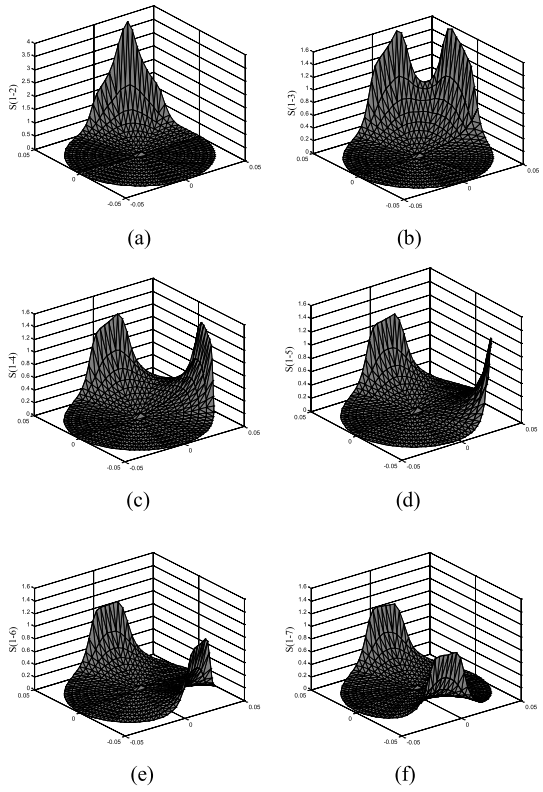

FIGURE 4. Six typical sensitivity distributions of CCERT sensor under the one-electrode excitation pattern. (a) Electrode pair 1-2. (b) Electrode pair 1-3. (c) Electrode pair 1-4. (d) Electrode pair 1-5. (e) Electrode pair 1-6. (f) Electrode pair 1-7.

B. TYPICAL SENSITIVITY DISTRIBUTIONS OF CCERT SENSOR UNDER THREE-ELECTRODE EXCITATION PATTERN

For the three-electrode excitation pattern, the five typical sensitivity distributions of the CCERT sensor are shown in Fig. 5.

C. TYPICAL SENSITIVITY DISTRIBUTIONS OF CCERT SENSOR UNDER FIVE-ELECTRODE EXCITATION PATTERN

For the five-electrode excitation pattern, the four typical sensitivity distributions of the CCERT sensor are shown in Fig. 6.

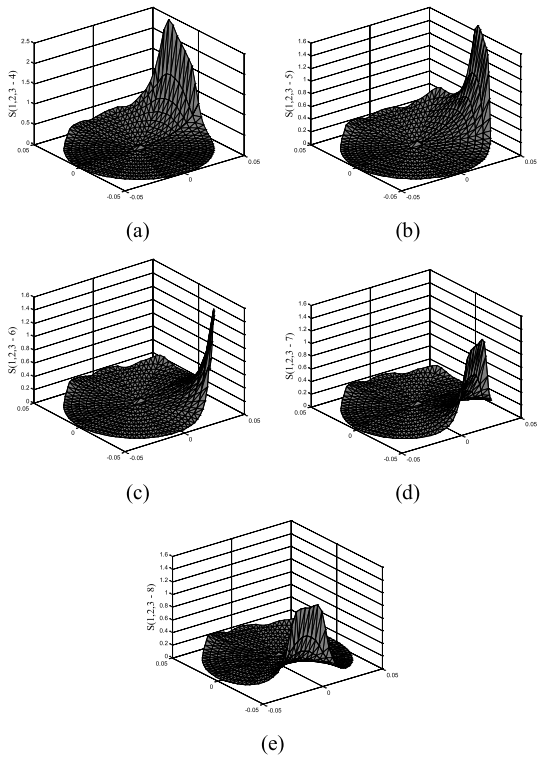

FIGURE 5. Five typical sensitivity distributions of CCERT sensor under the three-electrode excitation pattern. (a) Electrode pair 1, 2, 3-4. (b) Electrode pair 1, 2, 3-5. (c) Electrode pair 1, 2, 3-6. (d) Electrode pair 1, 2, 3-7. (e) Electrode pair 1, 2, 3-8.

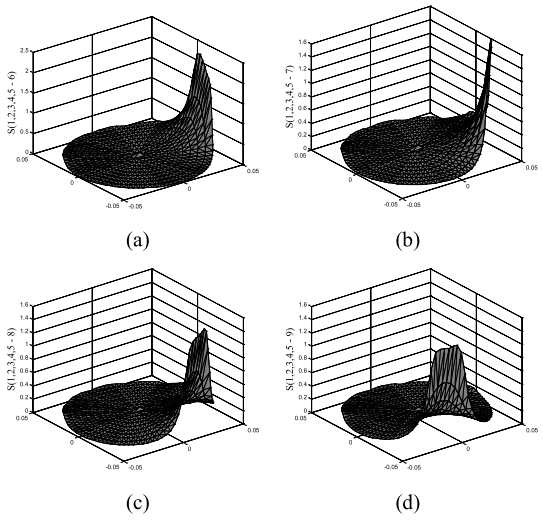

FIGURE 6. Four typical sensitivity distributions of CCERT sensor under the five-electrode excitation pattern. (a) Electrode pair 1, 2, 3, 4, 5-6. (b) Electrode pair 1, 2, 3, 4, 5-7. (c) Electrode pair 1, 2, 3, 4, 5-8. (d) Electrode pair 1, 2, 3, 4, 5-9.

D. DISCUSSIONS AND COMPARISONS

From Fig.4∼Fig.6, it can be found that there is no negative-sensitivity region in all the sensitivity distributions under the three excitation patterns. For all the sensitivity distributions

TABLE 1. Sensitivity distribution indices of the CCERT sensor under different excitation patterns.

Excitation pattern	S_{max}	S_{min}	$\overline{S}$	K_{a-b}	
				Adjacent	Opposite
One-electrode excitation pattern (a=1)	3.8916	0.0011	0.1620	898.7 (b=2)	15.7 (b=7)
Three-electrode excitation pattern (a=1,2,3)	2.5519	0.0050	0.1691	151.9 (b=4)	9.8 (b=8)
Five-electrode excitation pattern (a=1,2,3,4,5)	2.1840	0.0134	0.1718	54.0 (b=6)	8.9 (b=9)

under the three excitation patterns, there is no uniform sensitivity distribution. In each sensitivity distribution, sensitivities of the elements in the central area are all much lower than that of the elements near the wall. In the one-electrode excitation pattern, sensitivities of the elements near the excitation electrode are almost the same as that of the elements near the detection electrode. While, as the number of excitation electrodes increases, sensitivities of the elements near the detection electrode are increasing to be much higher than that of the elements near the excitation electrodes, especially in the five-electrode excitation pattern.

To quantitatively analyze the sensitivity distributions, four indexes, the average sensitivity $\overline{S}$, the maximum sensitivity S_{max}, the minimum sensitivity S_{min} and the uniformity coefficient K_{a-b}, are introduced.

The average sensitivity $\overline{S}$ is defined as:

$$\overline{S} = \frac{1}{N}\sum_{j=1}^{N}\overline{S}_j \tag{5}$$

where, N is the number of typical sensitivity distributions. For one-electrode excitation pattern, there are six typical distributions, $N = 6$. For three-electrode excitation pattern, there are five typical sensitivity distributions, $N = 5$. For five-electrode excitation pattern, there are four typical sensitivity distributions, $N = 4$. $\overline{S}_j = \frac{1}{M}\sum_{i=1}^{M} S^i_{a-b}$ is the average sensitivity of the jth typical sensitivity distribution, where $M = 864$ is the number of elements. Obviously, $\overline{S}$ is the overall average of all the typical sensitivity distributions of a specific excitation pattern.

The maximum sensitivity S_{max} is defined as

$$S_{max} = \max(S^j_{max}) \quad j = 1, 2, \ldots, N \tag{6}$$

where, $S^j_{max} = \max(S^i_{a-b})$ is the maximum sensitivity of the jth typical sensitivity distribution, $i = 1, 2, \ldots, M$. So, S_{max} is the maximum of all the typical sensitivity distributions of a specific excitation pattern.

Similarly, the minimum sensitivity S_{min} is defined as

$$S_{min} = \min(S^j_{min}) \quad j = 1, 2, \ldots, N \tag{7}$$

where, $S^j_{min} = \min(S^i_{a-b})$ is the minimum sensitivity of the jth typical sensitivity distribution, $i = 1, 2, \ldots, M$. So, S_{min} is the minimum of all the typical sensitivity distributions of a specific excitation pattern.

The uniformity coefficient of a specific typical sensitivity distribution K_{a-b} is determined by the ratio of the sum of 50 maximum sensitivities and the sum of 50 minimum sensitivities, which can be described as

$$K_{a-b} = S^{max\,50}_{a-b} / S^{min\,50}_{a-b} \tag{8}$$

where, $S^{max\,50}_{a-b}$ is the sum of 50 maximum sensitivities of the typical sensitivity distribution and $S^{min\,50}_{a-b}$ is the sum of 50 minimum sensitivities of the typical sensitivity distribution.

Uniformity coefficients of two typical sensitivity distributions (one is the distribution that the detection electrode is adjacent to the excitation electrode(s), the other is the distribution that the detection electrode is opposite to the excitation electrode(s)) under the three excitation patterns are compared, as shown in Table I. For the one-electrode excitation pattern with electrode 1 selected as the excitation electrode ($a = 1$), electrode 2 is the adjacent detection electrode ($b = 2$) and electrode 7 is the opposite detection electrode ($b = 7$). For the three-electrode excitation pattern with electrode 1, 2, 3 selected as the excitation electrodes ($a = 1$, 2 and 3), electrode 4 is the adjacent detection electrode ($b = 4$) and electrode 8 is the opposite detection electrode ($b = 8$). For the five-electrode excitation pattern with electrode 1, 2, 3, 4, 5 selected as the excitation electrodes ($a = 1$, 2, 3, 4 and 5), electrode 6 is the adjacent detection electrode ($b = 6$) and electrode 9 is the opposite detection electrode ($b = 9$).

Table I lists the four indexes of the CCERT sensor under different excitation patterns. It can be found that the CCERT sensor has the lowest average sensitivity under the one-electrode excitation pattern and has the highest average sensitivity under the five-electrode excitation pattern. That means with the increase of the number of excitation electrodes, the overall sensitivity of the CCERT sensor also increases. Meanwhile, for the detection electrode in either the adjacent position or the opposite position relative to the excitation electrode(s), the uniformity coefficient of sensitivity distribution under the one-electrode excitation pattern is the largest and that under the five-electrode excitation pattern is the smallest. Because smaller uniformity coefficient means better uniformity of sensitivity distribution, the research results indicate that with the increase of the number of excitation electrodes, the sensitivity distribution of the CCERT sensor becomes more uniform.

Although the measurement strategy of CCERT is different from that of the conventional ERT [9], [16], [17], [36], [37] and ECT [38], [39], some similar characteristics can be found, such as all of the sensitivity distributions are not uniform, the

sensitivities of the elements near the wall are much higher than that of the elements in the central area. Meanwhile, unlike some ERT sensors and some ECT sensors which have negative regions in the sensitivity distributions [10], [12], [36], [37], there is no negative region in the sensitivity distributions of the CCERT sensor. That is beneficial for succeeding image reconstruction and parameter measurement.

Although the increase of excitation electrodes result in higher average sensitivity and better distribution uniformity, from the viewpoint of practical application, with the increase of the excitation electrodes, the difficulty of sensor design and the complexity of the CCERT sensor will also increase, while the number of independent measurements may decrease.

IV. CONCLUSION

The sensitivity distributions of CCERT under three different excitation patterns (the one-electrode excitation pattern, the three-electrode excitation pattern and the five-electrode excitation pattern) were studied and compared by software simulation (COMSOL Multiphysics and MATLAB). The research results obtained in this work are listed as follows:

(1) There is no negative region exists in the sensitivity distributions of CCERT. That is beneficial for further image reconstruction and parameter measurement.

(2) The sensitivity distributions of CCERT are not uniform. The sensitivities of the elements near the pipe wall are much higher than that of the elements in the central area.

(3) With the increase of the number of excitation electrodes, the average sensitivity of the sensitivity distributions increases and the sensitivity distribution becomes more uniform.

Useful knowledge and experience are obtained in this work, which can provide reference for further research and development of CCERT. However, more research works should be undertaken in this area, such as how to make a suitable compromise between the sensitivity distribution, the system complexity of CCERT and the number of independent measurements, etc.

REFERENCES

[1] M. S. Beck, T. Dyakowski, and R. A. Williams, "Process tomography—The state of the art," *Trans. Inst. Meas. Control*, vol. 20, no. 4, pp. 163–177, Jan. 1998.

[2] M. S. Beck and R. A. Williams, "Process tomography: A European innovation and its applications," *Meas. Sci. Technol.*, vol. 7, no. 3, pp. 214–215, Jan. 1996.

[3] T. Dyakowski, "Process tomography applied to multi-phase flow measurement," *Meas. Sci. Technol.*, vol. 7, no. 3, pp. 343–353, Jan. 1996.

[4] M. Zhang, L. Ma, and M. Soleimani, "Magnetic induction tomography guided electrical capacitance tomography imaging with grounded conductors," *Measurement*, vol. 53, no. 7, pp. 171–181, Jul. 2014.

[5] Y. A. Wahab *et al.*, "Non-invasive process tomography in chemical mixtures—A review," *Sens. Actuators B, Chem.*, vol. 210, pp. 602–617, Apr. 2015.

[6] K. Wei and C.-H. Qiu, K. Primrose, "Super-sensing technology: Industrial applications and future challenges of electrical tomography," *Phil. Trans. R. Soc. A*, vol. 374, no. 2070, Jun. 2016, Art. no. 20150328.

[7] H. S. Tapp, A. J. Peyton, E. K. Kemsley, and R. H. Wilson, "Chemical engineering applications of electrical process tomography," *Sens. Actuators B, Chem.*, vol. 92, nos. 1–2, pp. 17–24, Jul. 2003.

[8] T. York, "Status of electrical tomography in industrial applications," *J. Electron. Imag.*, vol. 10, no. 3, pp. 608–619, Jul. 2001.

[9] T. Dyakowski, L. F. C. Jeanmeure, and A. J. Jaworski, "Applications of electrical tomography for gas–solids and liquid-solids flows—A review," *Powder Technol.*, vol. 112, no. 3, pp. 174–192, Oct. 2000.

[10] W. R. B. Lionheart, "EIT reconstruction algorithms: Pitfalls, challenges and recent developments," *Physiol. Meas.*, vol. 25, no. 1, pp. 125–142, Feb. 2004.

[11] C. G. Xie *et al.*, "Electrical capacitance tomography for flow imaging: System model for development of image reconstruction algorithms and design of primary sensors," *IEE Proc. G Circuits, Devices Syst.*, vol. 139, no. 1, pp. 89–98, Feb. 1992.

[12] D. Watzenig and C. Fox, "A review of statistical modelling and inference for electrical capacitance tomography," *Meas. Sci. Technol.*, vol. 20, no. 5, Apr. 2009, Art. no. 052002.

[13] S. R. Aw, R. A. Rahim, M. H. F. Rahiman, F. R. M. Yunus, and C. L. Goh, "Electrical resistance tomography: A review of the application of conducting vessel walls," *Powder Technol.*, vol. 254, pp. 256–264, Mar. 2014.

[14] M. Sharifi and B. Young, "Electrical resistance tomography (ERT) applications to chemical engineering," *Chem. Eng. Res. Design*, vol. 91, no. 9, pp. 1625–1645, Sep. 2013.

[15] M. Soleimani, H. G. Wang, Y. Li, and W. Yang, "A comparative study of 3D electrical capacitance tomography," *Int. J. Inf. Syst. Sci.*, vol. 3, no. 2, pp. 292–306, Jan. 2007.

[16] F. Dickin and M. Wang, "Electrical resistance tomography for process applications," *Meas. Sci. Technol.*, vol. 7, no. 3, pp. 247–260, Mar. 1996.

[17] R. Gadd, P. M. Record, and P. Rolfe, "Finite element modelling for electrical impedance tomography," in *Proc. 12th IEEE EMBS*, Orlando, FL, USA, 1990, pp. 133–134.

[18] M. Wang, F. J. Dickin, and R. A. Williams, "Electrical resistance tomography of metal walled vessels and pipelines," *Electron. Lett.*, vol. 30, no. 10, pp. 771–773, May 1994.

[19] Q. Zhu, W. R. B. Lionheart, F. J. Lidgey, C. N. McLeod, K. S. Paulson, and M. K. Pidcock, "An adaptive current tomograph using voltage sources," *IEEE Trans. Biomed. Eng.*, vol. 40, no. 2, pp. 163–168, Feb. 1993.

[20] M. Gevers, P. Gebhardt, S. Westerdick, M. Vogt, and T. Musch, "Fast electrical impedance tomography based on code-division-multiplexing using orthogonal codes," *IEEE Trans. Instrum. Meas.*, vol. 64, no. 5, pp. 1188–1195, May 2015.

[21] A. Adler, P. O. Gaggero, and Y. Maimaitijiang, "Adjacent stimulation and measurement patterns considered harmful," *Physiol. Meas.*, vol. 32, no. 7, pp. 731–744, Jul. 2011.

[22] L. Xiao, Q. Xue, and H. Wang, "Finite element mesh optimisation for improvement of the sensitivity matrix in electrical resistance tomography," *IET Sci., Meas. Technol.*, vol. 9, no. 7, pp. 792–799, Oct. 2015.

[23] W. Q. Yang, D. M. Spink, J. C. Gamio, and M. S. Beck, "Sensitivity distributions of capacitance tomography sensors with parallel field excitation," *Meas. Sci. Technol.*, vol. 8, no. 5, pp. 562–569, May 1997.

[24] W. R. B. Lionheart, J. Kaipio, and C. N. McLeod, "Generalized optimal current patterns and electrical safety in EIT," *Physiol. Meas.*, vol. 22, no. 1, pp. 85–90, Feb. 2001.

[25] P. J. Riu, J. R. Ferrer, and R. Pallas-Areny, "Multifrequency electrical impedance tomography as an alternative to absolute imaging," in *Tomographic Techniques for Process Design and Operation*, M. S. Beck, Ed. Southampton, U.K.: Computational Mechanics Publications, 1993, ch. 1.2, pp. 53–62, accessed on May 31, 2016. [Online]. Available: https://www.researchgate.net/publication/303689568

[26] J. C. Gamio, "A comparative analysis of single- and multiple-electrode excitation methods in electrical capacitance tomography," *Meas. Sci. Technol.*, vol. 13, no. 12, pp. 1799–1809, Nov. 2002.

[27] K. J. Alme and S. Mylvaganam, "Comparison of different measurement protocols in electrical capacitance tomography using simulations," *IEEE Trans. Instrum. Meas.*, vol. 56, no. 6, pp. 2119–2130, Dec. 2007.

[28] M. Mao, J. Ye, H. Wang, J. Zhang, and W. Yang, "Evaluation of excitation strategy with multi-plane electrical capacitance tomography sensor," *Meas. Sci. Technol.*, vol. 27, no. 11, Mar. 2016, Art. no. 114008.

[29] Z. Z. Yu, A. J. Peyton, L. A. Xu, and M. S. Beck, "Electromagnetic inductance tomography (EMT): Sensor, electronics and image reconstruction algorithm for a system with a rotatable parallel excitation field," *IEE Proc.-Sci., Meas. Technol.*, vol. 145, no. 1, pp. 20–25, Jan. 1998.

[30] X. Ma, A. J. Peyton, S. R. Higson, and P. Drake, "Development of multiple frequency electromagnetic induction systems for steel flow visualization," *Meas. Sci. Technol.*, vol. 19, no. 9, Sep. 2008, Art. no. 094008.

[31] Y. Fu, F. Dong, and C. Tan, "Response of the excitation condition to electromagnetic tomography," *Flow Meas. Instrum.*, vol. 31, pp. 10–18, Jun. 2013.
[32] H. Ji *et al.*, "A new dual-modality ECT/ERT technique based on C^4D principle," *IEEE Trans. Instrum. Meas.*, vol. 65, no. 5, pp. 1042–1050, May 2016.
[33] B. Wang, W. Zhang, Z. Huang, H. Ji, and H. Li, "Modeling and optimal design of sensor for capacitively coupled electrical resistance tomography system," *Flow Meas. Instrum.*, vol. 31, pp. 3–9, Jun. 2013.
[34] B. Wang, Y. Hu, H. Ji, Z. Huang, and H. Li, "A novel electrical resistance tomography system based on C^4D technique," *IEEE Trans. Instrum. Meas.*, vol. 62, no. 5, pp. 1017–1024, May 2013.
[35] K. Yee, "Numerical solution of initial boundary value problems involving Maxwell's equations in isotropic media," *IEEE Trans. Antennas Propag.*, vol. 14, no. 3, pp. 302–307, May 1966.
[36] P. Kauppinen, J. Hyttinen, and J. Malmivuo, "Sensitivity distribution visualizations of impedance tomography measurement strategies," *Int. J. Bioelectromagn.*, vol. 82, no. 1, pp. VII-1–VII-9, Jan. 2006.
[37] C. Rücker and T. Günther, "The simulation of finite ERT electrodes using the complete electrode model," *Geophysics*, vol. 76, no. 4, pp. F227–F238, Jul. 2011.
[38] Ø. Isaksen, "A review of reconstruction techniques for capacitance tomography," *Meas. Sci. Technol.*, vol. 7, no. 3, pp. 325–337, Mar. 1996.
[39] W. Q. Yang and L. Peng, "Image reconstruction algorithms for electrical capacitance tomography," *Meas. Sci. Technol.*, vol. 14, no. 1, p. R1, Jan. 2003.

ZHEN XU was born in Wuxi, China, in 1993. He received the B.Sc. degree from the Huazhong University of Science and Technology, Wuhan, China, in 2016. He is currently pursuing the Ph.D. degree with the College of Control Science and Engineering, Zhejiang University, Hangzhou, China. His current research interests include process tomography, multiphase flow measurement, and automation instrumentation.

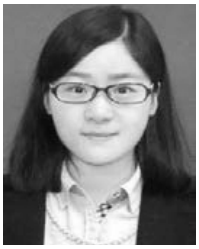

YANDAN JIANG was born in Jinhua, China, in 1992. She received the B.Sc. degree from the Zhejiang University of Technology, Hangzhou, China, in 2013. She is currently pursuing the Ph.D. degree with the College of Control Science and Engineering, Zhejiang University, Hangzhou. Her current research interests include automation instrumentation, multiphase flow measurement, ultrasound-based and electrical-based sensors, and industrial process tomography.

BAOLIANG WANG was born in Zibo, China, in 1970. He received the B.Sc. and M.Sc. degrees from the Shandong University of Technology, Jinan, China, in 1992 and 1995, respectively, and the Ph.D. degree from Zhejiang University, Hangzhou, China, in 1998. From 1998 to 2001, he was a Lecturer with the Department of Control Science and Engineering, Zhejiang University. From 2002 to 2003, he was a Research Associate with the City University of Hong Kong. From 2002 to 2013, he was an Associate Professor and since 2014, he has been a Professor with the Department of Control Science and Engineering, Zhejiang University. His research interests include process tomography, motion control system, and microprocessor application.

ZHIYAO HUANG was born in Hangzhou, China, in 1968. He received the B.Sc., M.Sc., and Ph.D. degrees from Zhejiang University, Hangzhou, in 1990, 1993, and 1995, respectively. From 1995 to 1997, he was a Lecturer with the Department of Chemical Engineering, Zhejiang University. In 1997, he became an Associate Professor with the Department of Control Science and Engineering, Zhejiang University, and in 2001, he was appointed a Professor. Currently, he is a Professor with the College of Control Science and Engineering. He is also a permanent staff with the State Key Laboratory of Industrial Control Techniques. His current research interests include automation instrumentation and multiphase flow measurement.

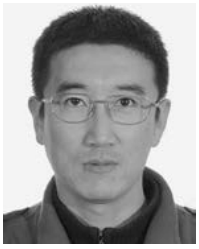

HAIFENG JI was born in Shijiazhuang, China, in 1973. He received the M.Sc. degree from the Shandong University of Technology, Jinan, China, in 1999, and the Ph.D. degree from the Department of Control Science and Engineering, Zhejiang University, Hangzhou, China, in 2002. He is currently an Associate Professor with the Department of Control Science and Engineering, Zhejiang University. His research interests include measurement techniques, automation equipment, information processing of complex process system, and multiphase flow measurement in mini-/micro-channel.

HAIQING LI received the B.Sc. degree from Dalian Science and Engineering University, Dalian, China, in 1956. From 1988 to 1997, she was a Professor with the Department of Chemical Engineering, Zhejiang University, where she has been a Professor with the Department of Control Science and Engineering, since 1997. Her research interests include automation instrumentation and multiphase flow measurement.